Bayesian Estimation Approach using MCMC for Model Identification of Glucose-Insulin Dynamics for Type 1 Diabetes: A Simulation and Experimental Study

Milad Ghanbari

1 Introduction

Diabetes mellitus is a group of metabolic diseases characterized by chronic hyperglycemia resulting from defects in insulin secretion, insulin action, or both [1]. Diabetes is a major cause of many diseases like kidney failure, blindness, stroke, heart attacks, and lower limb amputation. The most common type of diabetes among children and youth is type 1 diabetes [2]. Type 1 diabetes is a chronic and autoimmune disease in which the pancreas (an organ that produces insulin in order to regulate blood glucose) secretes insufficient amount of insulin. This leads to an accumulation of blood sugar, also known as hyperglycemia [3]. Insulin treatment strategies in type 1 diabetes include either multiple daily insulin injections or continuous subcutaneous insulin infusion with an insulin pump [4]. Insulin therapy uses two types of subcutaneous insulin named basal and bolus. Basal insulin is the slow acting one, which compensates glycemia rising caused by endogenous glucose production. Bolus insulin is fast acting and used to compensate glycemia rise due to meal intake. Automating the process of insulin replacement in type 1 diabetes from blood glucose monitoring to insulin delivery controlled by a mathematical algorithm became known as closed-loop control of diabetes, or the artificial pancreas [5].

Having a mathematical model describing glucose-insulin dynamics can be useful in the field of diabetes for both simulation and control. Several models have been developed and can be found in the literature. It started with Himsworth and Ker [6] introducing the first approach to measure the insulin sensitivity. Among all the developed models, Bergman and Hovorka models are the most well-known models. Bergman and co-workers proposed a minimal model consisting three compartments to analyze the glucose disappearance and insulin sensitivity during an intravenous glucose tolerance test [7]. Extension of the minimal model including three insulin and glucose subcompartments for capturing absorption, distribution, and disposal dynamics was introduced by Hovorka and colleagues [8]. Hovorka model will be utilized in this project.

In this report, a nonlinear identification technique is applied to identify the model of glucose-insulin dynamics using both experimental and simulation data. The report is organized as follows. In section 2, Hovorka model (a well-known nonlinear model describing glucose-insulin dynamics) is described. In section 3, the necessary assumptions and considerations for simulation environment are discussed. In section 4, the details of the experimental data collected from a patient with type 1 diabetes are provided. In section 5, the selected identification technique for this application is discussed. Finally, in the last section, the glucose-insulin model is identified using the designed approach and data, followed by providing results and appropriate discussion on them.

2 Nonlinear Model

Hovorka model [8] is a nonlinear compartment model with two inputs (insulin and meal intake) and one output (blood glucose levels). Model is divided into four submodels: gut glucose absorption, insulin absorption, insulin action, and glucose kinetics. In practice, a continuous glucose monitoring (CGM) is used as the sensor to measure blood glucose levels, then a sensor model is included as another submodel of the system. In the following each one of these submodels are described.

2.1 Submodel of Glucose Kinetics

The glucose kinetics is represented by a two-compartment submodel that describes the distribution, production, and utilization of glucose and its control by insulin. The submodel of glucose kinetics is described as:

$$\frac{dQ_1(t)}{dt} = -[\frac{F_{01}}{V * G(t)} + x_1(t)]Q_1(t) + k_{12}Q_2(t) + EGP + U_m \tag{1}$$

$$\frac{dQ_2(t)}{dt} = x_1(t)Q_1(t) - [k_{12} + x_2(t)]Q_2(t) \tag{2}$$

$$EGP = \begin{cases} EGP_0(1 - x_3(t)) & : x_3(t) < 1 \\ 0 & : x_3(t) \geq 1 \end{cases} \tag{3}$$

$$G(t) = \frac{Q_1(t)}{V} \tag{4}$$

where $Q1$, $Q2$ (μmol/kg) represent the masses of glucose in the accessible (where glycemia measurements are made) and non-accessible compartments,respectively. k_{12} (1/min) is the transfer rate parameter, F_01 (μmol/kg/min) is the non-insulin dependent glucose utilization, and EGP_0 (μmol/kg/min) is the endogenous glucose production extrapolated to zero insulin concentration. G (mmol/L) is the plasma glucose concentration and V (ml/kg) is the glucose distribution volume.

2.2 Submodel of Insulin Action

The insulin action submodel includes three remote effects of insulin on glucose kinetics: (i) the effect on glucose transport/distribution, (ii) glucose disposal, and (iii) endogenous glucose production. The submodel of insulin action is described as:

$$\frac{dx_1(t)}{dt} = -k_{a1}x_1(t) + k_{a1}S_tI_p(t) \tag{5}$$

$$\frac{dx_2(t)}{dt} = -k_{a2}x_2(t) + k_{a2}S_dI_p(t) \tag{6}$$

$$\frac{dx_1(t)}{dt} = -k_{a3}x_3(t) + k_{a3}S_eI_p(t) \tag{7}$$

where x_1, x_2, and x_3 (1/min) are the remote effects of insulin on glucose distribution, glucose disposal, and the endogenous glucose production, respectively, k_{a1}, k_{a2}, and k_{a3} (1/min) are time constants, S_t and S_d (1/(min mU/l)) are the insulin sensitivities of glucose distribution and glucose disposal, respectively, and S_e (1/(mU/l)) is the insulin sensitivity of endogenous glucose production.

2.3 Submodel of Insulin Absorption

The submodel of insulin absorption is represented by three compartments with the insulin divided into an accessible and nonaccessible compartment. The submodel of insulin absorption is described as:

$$\frac{dQ_{i1}(t)}{dt} = u_i(t) - \frac{Q_{i1}(t)}{t_{max}} \tag{8}$$

$$\frac{dQ_{i2}(t)}{dt} = \frac{Q_{i1}(t)}{t_{max}} - \frac{Q_{i2}(t)}{t_{max}} \tag{9}$$

$$\frac{dQ_i(t)}{dt} = -\frac{Q_i(t)}{t_p} + \frac{Q_{i2}(t)}{t_{max}} \tag{10}$$

$$I_p(t) = \frac{Q_i(t)}{w.V_i} * 10^6 + I_b \tag{11}$$

where Q_{i1} and Q_{i2} (units) represent insulin masses in the accessible and nonaccessible compartments, u_i (unit/min) represents administration (bolus and infusion) of insulin, t_{max} (min) represents insulin absorption rate constant, V_i (ml/kg) is the volume of distribution of rapid-acting insulin, I_p is the insulin concentration in plasma, I_b (mU/l) is the background plasma insulin concentration , and t_p (min) represents the fractional elimination rate from plasma.

2.4 Submodel of Gut Glucose Absorption

The physiology of the gut absorption is represented by a two-compartment chain with identical fractional transfer rates. The submodel of gut glucose absorption is described as:

$$\frac{dQ_{m1}(t)}{dt} = u_m(t) - \frac{Q_{m1}(t)}{t_{mmax}} \tag{12}$$

$$\frac{dQ_{m2}(t)}{dt} = \frac{Q_{m1}(t)}{t_{mmax}} - \frac{Q_{m2}(t)}{t_{mmax}} \tag{13}$$

$$U_m(t) = \frac{Q_{m2}(t)}{t_{mmax}} \tag{14}$$

where Q_{m1} and Q_{m2} (μmol/kg) are the glucose masses in the first and second gut compartments, respectively, u_m (μmol/min) is the amount of ingested glucose, t_{mmax} (min) is time-to-peak appearance rate of glucose, and U_m (μmol/kg/min) is the gut absorption rate.

2.5 Submodel of Sensor

This submodel can be represented by:

$$\frac{dG_s(t)}{dt} = -k_s G_s(t) + k_s G(t) \tag{15}$$

where G_s (mmol/L) is the interstitial glucose concentration and k_s (1/min) is the time constant.

3 Simulation Environment

The Hovorka model introduced in section 2 was implemented in Matlab to construct a virtual closed-loop insulin delivery system. The created simulation is used to generate glucose-insulin data. In order to create a virtual patient and select realistic parameters, model parameters for simulation have been chosen from experimental studies [7] shown in Table 1. In the simulation, a white noise was added in glucose measurements with a coefficient of variation of 7%. The controller implemented in the closed-loop is the model predictive control (MPC) algorithm. The sample time was set to 10 minutes. Every 10 minutes, the MPC algorithm calculates the optimal basal insulin. Fig. 1 shows a simulated data having two meals. Sensor glucose levels, basal insulin, and information related to meals and boluses are provided in Fig. 1.

4 Experimental Data

Experimental data from a real patient with type 1 diabetes using subcutaneous pump therapy who participated in a clinical research study conducted at the McGill University Health Centre are used. Participant was admitted for a period of 9 hours from 8 am until 5 pm. Fig. 2 shows the experimental data including sensor glucose levels, basal insulin, and information related to the consumed meals and injected boluses for each meal. A model predictive controller algorithm was implemented to adjust the basal rates every 10 minutes.

Table 1: The model parameters selected for simulation extracted from experimental studies

Parameter	Value	Parameter	Value
t_{max} **(min)**	65	S_d **(1/(min mU/l))**	0.0001
t_p **(min)**	8.5	S_e **(1/(mU/l))**	0.014
I_b **(mU/l)**	0.2	t_{mmax} **(min)**	35
k_{a1} **(1/min)**	0.003	EGP_0 **(μmol/kg/min)**	25
k_{a2} **(1/min)**	0.09	F_{01} **(μmol/kg/min)**	18
k_{a3} **(1/min)**	0.04	k_{12} **(1/min)**	0.02
S_t **(1/(min mU/l))**	0.0015	k_s **(1/min)**	0.06

Table 2: Prior distribution of the model parameters extracted from experimental studies

Parameter	Distribution	Parameter	Distribution
t_{max}	$\mathcal{N}(55, (13)^2)$	S_d	$\mathcal{N}(0.0005, (0.0001)^2)$
t_p	$\mathcal{N}(9, (2.4)^2)$	S_e	$\mathcal{N}(0.019, (0.005)^2)$
I_b	$\mathcal{N}^+(0, (0.4)^2)$	t_{mmax}	$\mathcal{N}(45, (15)^2)$
k_{a1}	$\mathcal{N}(0.0034, (0.00085)^2)$	EGP_0	$\mathcal{N}(16.9, (4.2)^2)$
k_{a2}	$\mathcal{N}(0.056, (0.018)^2)$	F_{01}	$\mathcal{N}(11.1, (3.7)^2)$
k_{a3}	$\mathcal{N}(0.024, (0.006)^2)$	k_{12}	$\mathcal{N}(0.06, (0.015)^2)$
S_t	$\mathcal{N}(0.001841, (0.0006)^2)$	k_s	$\mathcal{N}(0.093, (0.024)^2)$

5 Identification Approaches

A nonlinear identification technique was chosen in order to identify the model of glucose-insulin dynamics for type 1 diabetes. We approach the problem of identifying nonlinear Hovorka model using Bayesian parameter estimation method implemented by Markov Chain Monte Carlo (MCMC). The details of his approach is provided in the next subsection.

5.1 Bayesian Parameter Estimation

In this section, we discuss the details of estimating the parameters of the nonlinear Hovorka model using Bayesian approach. The key quantity in Bayesian parameter estimation is the a posteriori probability density function of the unknown model parameters. From this function, which provides a complete description of the shape of the estimate uncertainty, the 95% confidence intervals can be derived. Obtaining the a posteriori probability density function of the unknown model parameters is a task that is analytically intractable because of the complex relationships between parameters and data. Therefore, MCMC was used to obtain the a posteriori probability density function. In overall, for the MCMC 6000 iterations were run. To allow the MCMC to stabilize, the first 1000 iterations were dropped out.

Approaches like nonlinear least squares and maximum likelihood face identifiability issue for the current parameter estimation problem [10]. Using Bayesian approach with appropriate selection of prior knowledge regarding unknown parameters can prevent identifiability issue. The prior distribution of model parameters are shown in Table 2. To assure nonnegativity of the parameters, all of them were log-transformed for implementation. These prior information were extracted from previous experimental studies on real subjects [7, 11, 12, 13, 14].

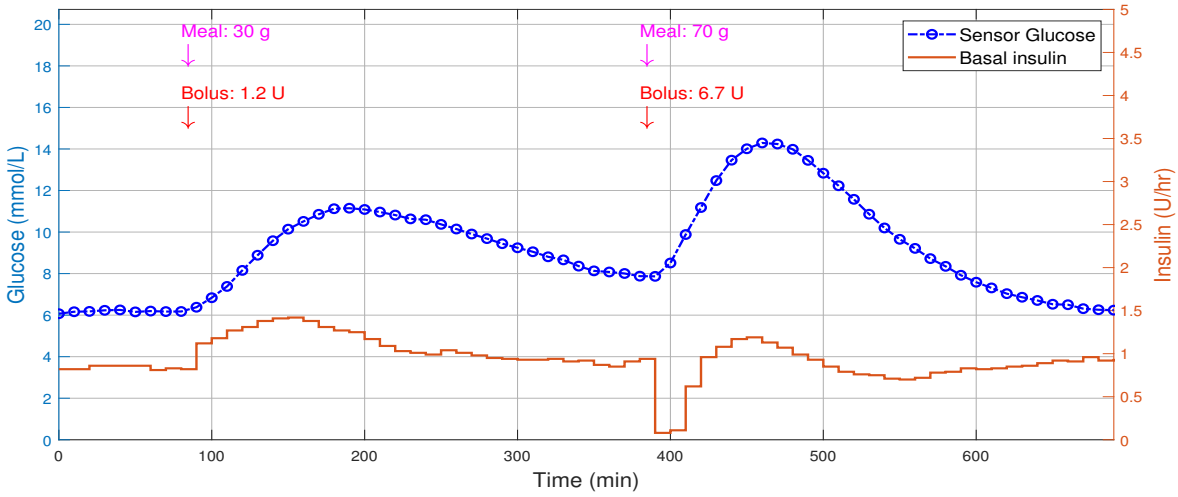

Figure 1: Data of a virtual patient from simulation

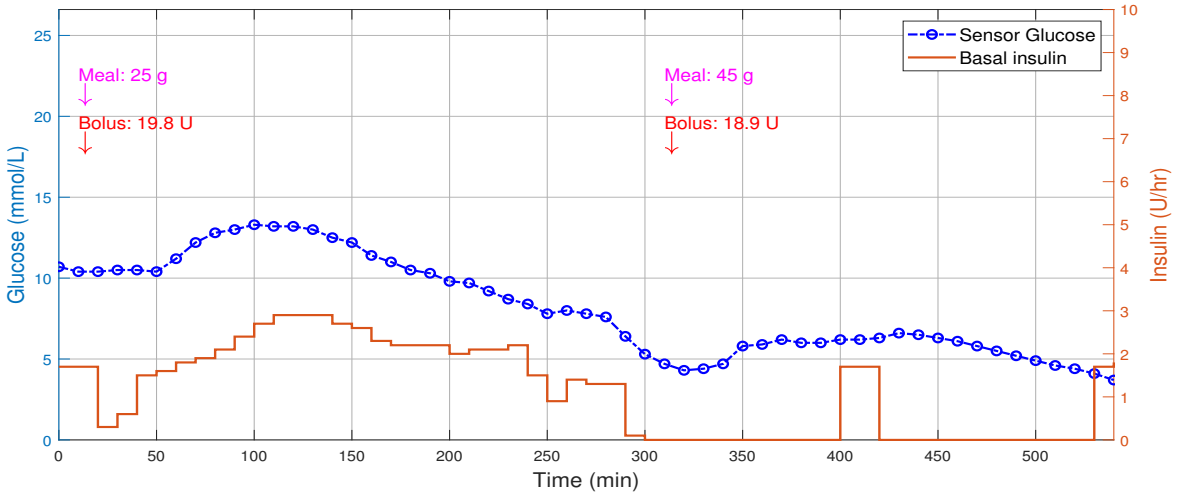

Figure 2: Experimental data of the real patient

6 Results and Discussion

In this section, the results of model identification using the discussed approach is provided. A sample model fit to glucose concentrations using simulation data and Bayesian approach implemented by MCMC is shown in Fig. 3. The figure reveals the goodness of model fit using Bayesian approach. Table 3 reports the parameters distribution of the Hovorka model estimated by Bayesian estimator and MCMC algorithm. As can be seen in this table, the median of the parameter estimates are quite close to the real parameters used for the simulation shown in Table 1. Moreover, the interquartile ranges of the parameter estimates are narrow indicating accurate estimation.

In order to study the effect of different noise levels on the parameter estimates with Bayesian estimator, one low level noise with CV of 2% and one moderate level noise with CV of 9% were applied. Fig. 4 and Fig. 5 show the results of this study on parameter estimates. In order to show all the ranges on the same figure in each study, the distribution ranges were normalized (divided by the median of each range). As can be seen from these graphs, interquartile ranges of parameter estimates increase by increasing the level of noise. In Fig. 4 and Fig. 5, numbers

shown on the vertical axis correspond to the following parameters vector:

$$\Theta = [t_{max} \quad t_p \quad I_b \quad k_{a1} \quad k_{a2} \quad k_{a3} \quad S_t \quad S_d \quad S_e \quad t_{mmax} \quad EGP_0 \quad F_{01} \quad k_{12} \quad k_s] \tag{16}$$

In order to evaluate the effectiveness of the designed identification approach, experimental data described in section 4 is used. Fig. 6 shows the models fit to glucose concentration measured from a real type 1 diabetes patient. Assessment of model fit is investigated by calculating the variance accounted for (VAF) in the all implemented identification scenarios reported in Table 4. Based on the table, a lower performance is achieved on experimental data compared to simulation data, possibly due to the unmodeled behaviors in glucose dynamics.

Posterior distributions of parameter estimates obtained from MCMC in the experimental study are shown in Fig. 7. The posterior distribution contains information about the mean and median as well as associated uncertainty. Measures of uncertainty such as the 95% credible intervals can be extracted from the posterior distribution. Comparing these graphs with Table 3, it can be seen that the parameter estimates in experimental case have wider interquartile ranges compared to the simulation case. The mentioned reason explains the wider range of confidence interval in glucose estimation in Fig. 6 (experimental case) compared to Fig. 3 (simulation case).

In conclusion, the problem of identifying the glucose-insulin dynamics of type 1 diabetes was tackled by designing and evaluating a nonlinear identification approach on both simulation and experimental data. Bayesian estimation technique and MCMC algorithm were considered for the designed approach. Based on the provided results and performance measures, the effectiveness of Bayesian approach on both simulation and experimental scenarios was seen. Furthermore, it was investigated and shown that level of noise has an important effect on the interquartile ranges of parameter estimates by Bayesian approach. An increase in the confidence interval range and decrease in performance (accuracy) of glucose estimation were seen in experimental case compared to simulation scenario. Choosing among variety of parameter estimators highly depends on the purpose of use and required accuracy. For instance, in order to design a simulator to mimic the behavior of a type 1 diabetes patient, the most accurate approach should be selected. On the other hand, for the online control purposes which calculating time or time complexity is crucial, a faster estimator with lower level of accuracy is acceptable.

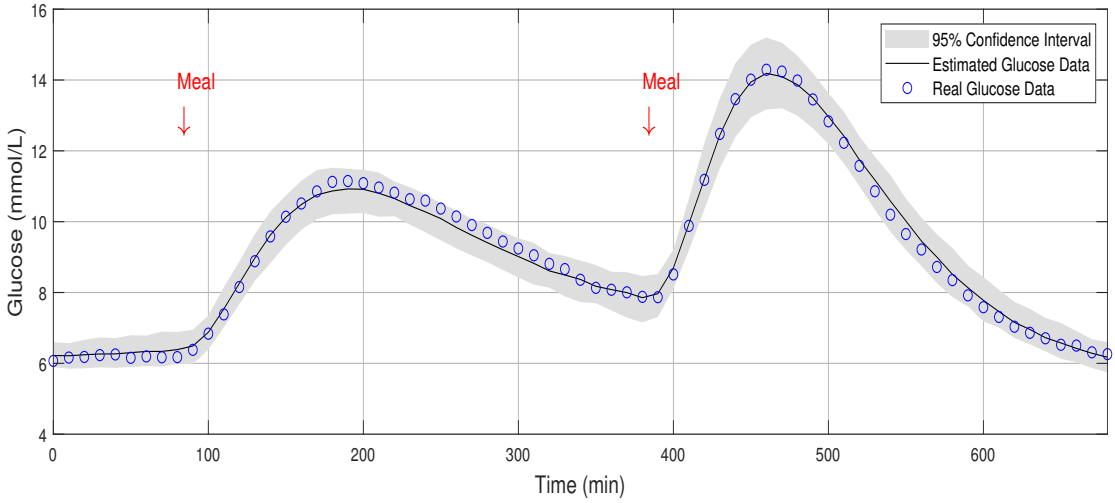

Figure 3: Sample model fit (median ± IQR) of glucose measured from a simulation study using Bayesian approach (the details of the data discussed in section 3)

Table 3: The model parameters estimated by Bayesian approach. The data are shown in median (interquartile range)

Parameter	median (IQR)	Parameter	median (IQR)
t_{max} **(min)**	65.26 (55.96 - 74.56)	S_d **(1/(min mU/l))**	0.0001 (0.000082 - 0.000118)
t_p **(min)**	8.4 (7.1 - 9.7)	S_e **(1/(mU/l))**	0.0153 (0.0137 - 0.0168)
I_b **(mU/l)**	0.23 (0.193 - 0.266)	t_{mmax} **(min)**	34.6 (30.10 - 39.09)
k_{a1} **(1/min)**	0.0029 (0.0026 - 0.0032)	EGP_0 **(μmol/kg/min)**	25.9 (22.27 - 29.52)
k_{a2} **(1/min)**	0.1114 (0.098 - 0.1248)	F_{01} **(μmol/kg/min)**	18.4 (16.01 - 20.79)
k_{a3} **(1/min)**	0.0439 (0.0369 - 0.0509)	k_{12} **(1/min)**	0.024 (0.0214 - 0.0266)
S_t **(1/(min mU/l))**	0.0016 (0.0014 - 0.0018)	k_s **(1/min)**	0.053 (0.045 - 0.0609)

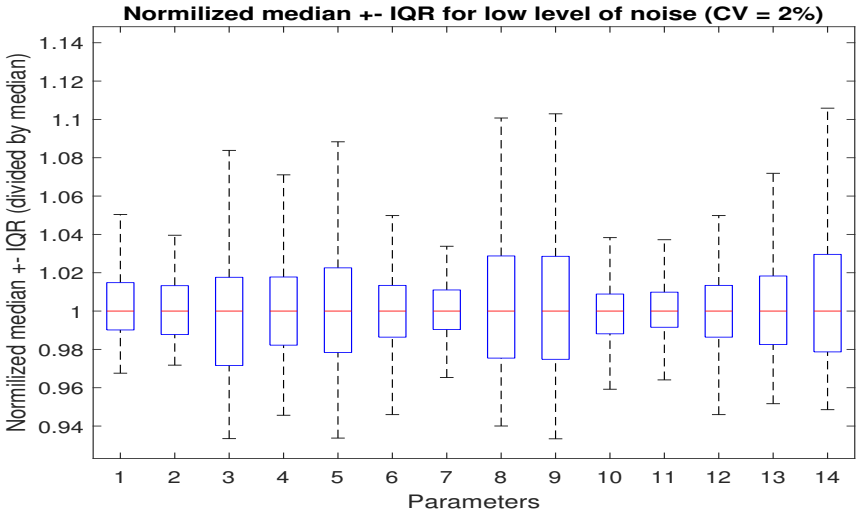

Figure 4: Estimated parameters distribution shown in normalized median ± IQR for low level of noise (CV = 2%)

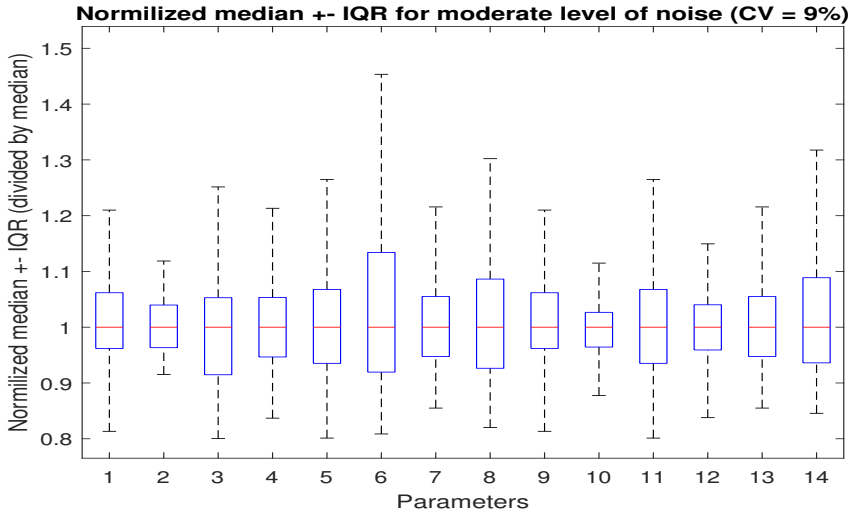

Figure 5: Estimated parameters distribution shown in normalized median ± IQR for moderate level of noise (CV = 9%)

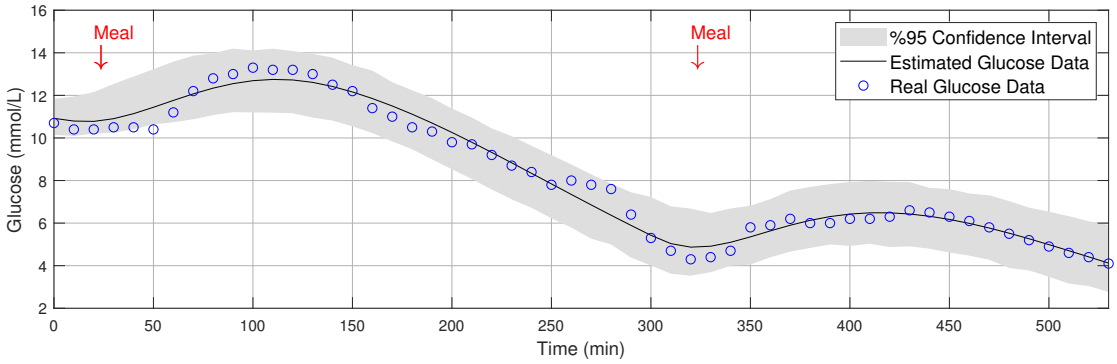

Figure 6: Sample model fit (median ± IQR) of glucose measured from a real patient (experimental data)

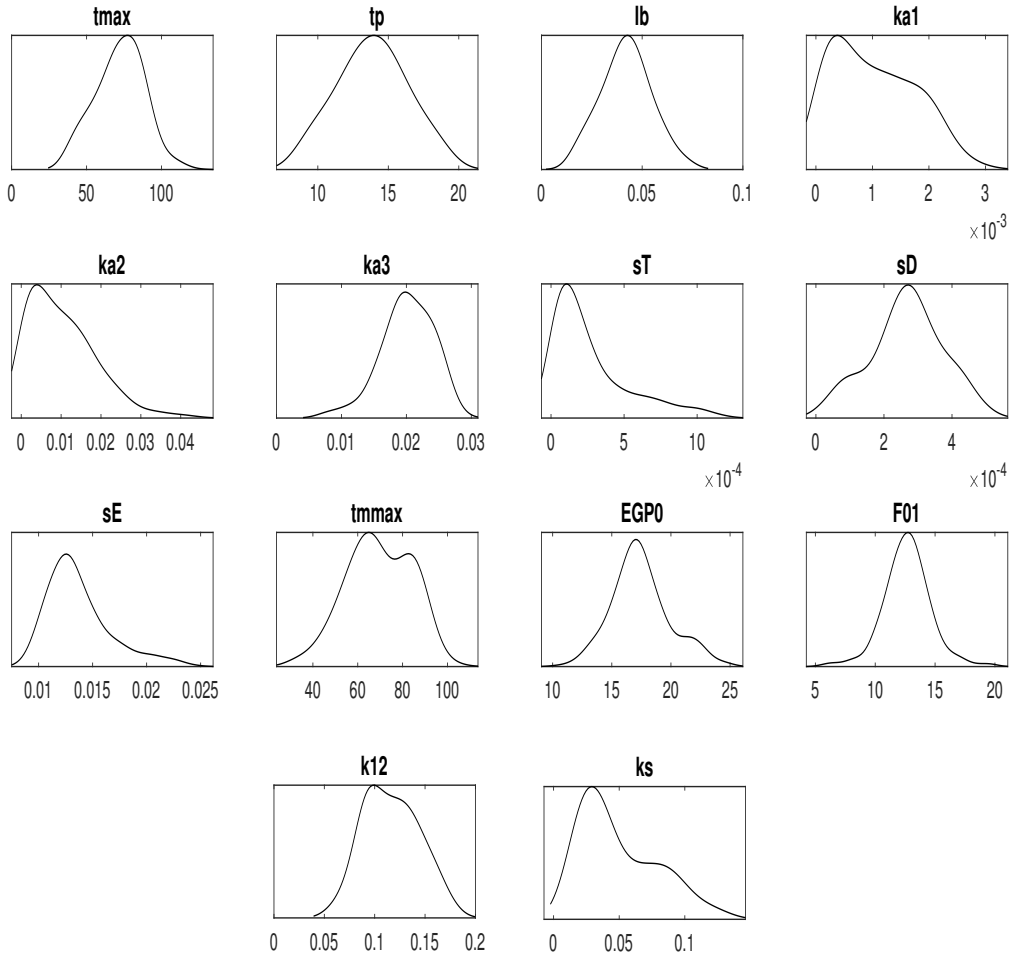

Figure 7: Posterior distribution of the estimated parameters related to the real patient

Table 4: Variance accounted for (VAF) in the different implemented identification scenarios

	Simulation data	**Experimental data**
Bayesian approach	98.2 %	91.37 %

References

[1] American Diabetes Association. "Diagnosis and classification of diabetes mellitus." Diabetes care 37.Supplement 1 (2014): S81-S90.

[2] Craig, Maria E., Andrew Hattersley, and Kim C. Donaghue. "Definition, epidemiology and classification of diabetes in children and adolescents." Pediatric diabetes 10 (2009): 3-12.

[3] Todd, John A. "Etiology of type 1 diabetes." Immunity 32.4 (2010): 457-467.

[4] Jeitler, K., et al. "Continuous subcutaneous insulin infusion versus multiple daily insulin injections in patients with diabetes mellitus: systematic review and meta-analysis." (2008): 941-951.

[5] Cobelli, Claudio, Eric Renard, and Boris Kovatchev. "Artificial pancreas: past, present, future." Diabetes 60.11 (2011): 2672-2682.

[6] Himsworth, H. P., and R. B. Kerr. "Insulin-sensitive and insulin-insensitive types of diabetes mellitus." Clinical Science 4 (1939): 119-152.

[7] Bergman, Richard N. "The minimal model of glucose regulation: a biography." Mathematical Modeling in Nutrition and the Health Sciences. Springer, Boston, MA, 2003. 1-19.

[8] Hovorka, Roman, et al. "Partitioning glucose distribution/transport, disposal, and endogenous production during IVGTT." American Journal of Physiology-Endocrinology and Metabolism 282.5 (2002): E992-E1007.

[9] Magdelaine, Nicolas, et al. "A long-term model of the glucose–insulin dynamics of type 1 diabetes." IEEE Transactions on Biomedical Engineering 62.6 (2015): 1546-1552.

[10] Pillonetto, Gianluigi, Giovanni Sparacino, and Claudio Cobelli. "Numerical non-identifiability regions of the minimal model of glucose kinetics: superiority of Bayesian estimation." Mathematical biosciences 184.1 (2003): 53-67.

[11] Wilinska, Malgorzata E., et al. "Insulin kinetics in type-1 diabetes: continuous and bolus delivery of rapid acting insulin." IEEE Transactions on Biomedical Engineering 52.1 (2004): 3-12.

[12] Hovorka, Roman, et al. "Nonlinear model predictive control of glucose concentration in subjects with type 1 diabetes." Physiological measurement 25.4 (2004): 905.

[13] Haidar, Ahmad, et al. "Stochastic virtual population of subjects with type 1 diabetes for the assessment of closed-loop glucose controllers." IEEE Transactions on Biomedical Engineering 60.12 (2013): 3524-3533.

[14] Wilinska, Malgorzata E., et al. "Simulation environment to evaluate closed-loop insulin delivery systems in type 1 diabetes." Journal of diabetes science and technology 4.1 (2010): 132-144.